Electronic Supplementary Material (ESI) for ChemComm.

Ce-induced regulation of electron density enhanced the catalytic activity of Co-Mn oxides for water oxidation

Wang Wang, Youcheng Hu, Shengli Chen*

Hubei Electrochemical Power Sources Key Laboratory, Department of Chemistry, Wuhan University, Wuhan 430072, China. Email: slchen@whu.edu.cn

Experimental section

Materials and Reagent: The following chemicals were used as received without any further purification: $Co(NO_3)_2 \cdot 6H_2O$ (99%, Sinopharm Chemical Reagent Co. Ltd), $Ce(NO_3)_3 \cdot 6H_2O$ (99%, Sinopharm Chemical Reagent Co. Ltd), KOH (99%, Sinopharm Chemical Reagent Co. Ltd), $Mn(NO_3)_2$ 50% aqueous solution (Sinopharm Chemical Reagent Co. Ltd), Ethanol (95%, Sinopharm Chemical Reagent Co. Ltd).

Synthesis: Typically, a piece of Ti mesh (2 cm x 1 cm) was firstly washed in ethanol and UP water for 15 minutes by ultrasonication. A 40 ml solution containing 0.2 mol/L Co^{2+} and 0.1 mol/L Mn^{2+} was used as electrolyte for the electrodeposition of the CMO. For the electrodeposition of CMCO, 14 mg of $Ce(NO_3)_3 \cdot 6H_2O$ was added to the above solution. For the electrodeposition, the Ti mesh was immersed into the electrolyte (1 cm^2) and used as the working electrode; the graphite rod was used as the counter electrode. The electrodeposition was conducted at a current of 4.5 mA for 120 seconds. After electrodeposition, the Ti mesh was washed with UP water and annealed at 350℃ in air for 2 h to obtain the catalysts.

Characterization: Powder X-ray diffraction (XRD) patterns were performed on a Smartlab SE X-ray diffractometer with a Cu Kα radiation source. The morphologies and sizes of the samples were observed by using a Zeiss Merlin Compact scanning electron microscope (SEM) and a FEI Tecnai G2 F20 transmission electron microscope (TEM). X-ray photoelectron spectroscopy (XPS) measurement was carried out with a Thermo Fischer Nexsa spectrophotometer.

Electrochemical Measurements: the electrochemical properties of all samples were measured by using a CHI 760E electrochemical analyzer (CH Instruments, Chenhua Co., Shanghai, People's Republic of China) in a three-electrode system at 25 ± 1℃. A freshly made reversible hydrogen electrode and a graphite rod were used as the working electrode, reference electrode, and counter electrode, respectively. The potentials were reported with respect to the reversible hydrogen electrode (RHE). The LSV curves were recorded at a scan rate of 5 mV/s. The CV curves were recorded at a scan rate of 50mV/s. Solutions of 1 M KOH was used as the electrolytes.

DFT calculations: the DFT calculations of spin-polarization in this article were performed by the Vienna ab initio simulation package (VASP) [1,2] with the generalized gradient approximation (GGA) of Perdew–Burke–Ernzerhof (PBE) [3]. A plane-wave energy cut-off of 400 eV was used in the expansion of the electronic wave function and the convergence threshold was 10^{-5} eV in energy and

0.05 eV/ Å in force for electronic relaxation and ion relaxation, respectively. Hubbard correction [4] was included because of the existence of transition metal oxide with a U value of 4.0 eV and 2.0 eV for Mn and Co, respectively. [5] Monkhorst-Pack k points is 2×2×1 for all the structures considered in this paper with gamma method for all the calculations in the article. The vacuum space of all the structures in the article was set 15 Å. For Co_2MnO_4 and Ce doped Co_2MnO_4, (110) plane is chosen. The computational hydrogen electrode (CHE) model [6] which used half of the chemical potential of H_2 instead of the chemical potential of H^+ was used to calculate proton-coupled electron transfer (PCET) thermodynamics of the oxygen evolution reactions in these structures. The entropies and zero-point-energies (ZPE) of H_2 molecule, H_2O molecule and ZPE of adsorbed oxygenated species ($*O_xH_y$) were referred to the literature. [6]

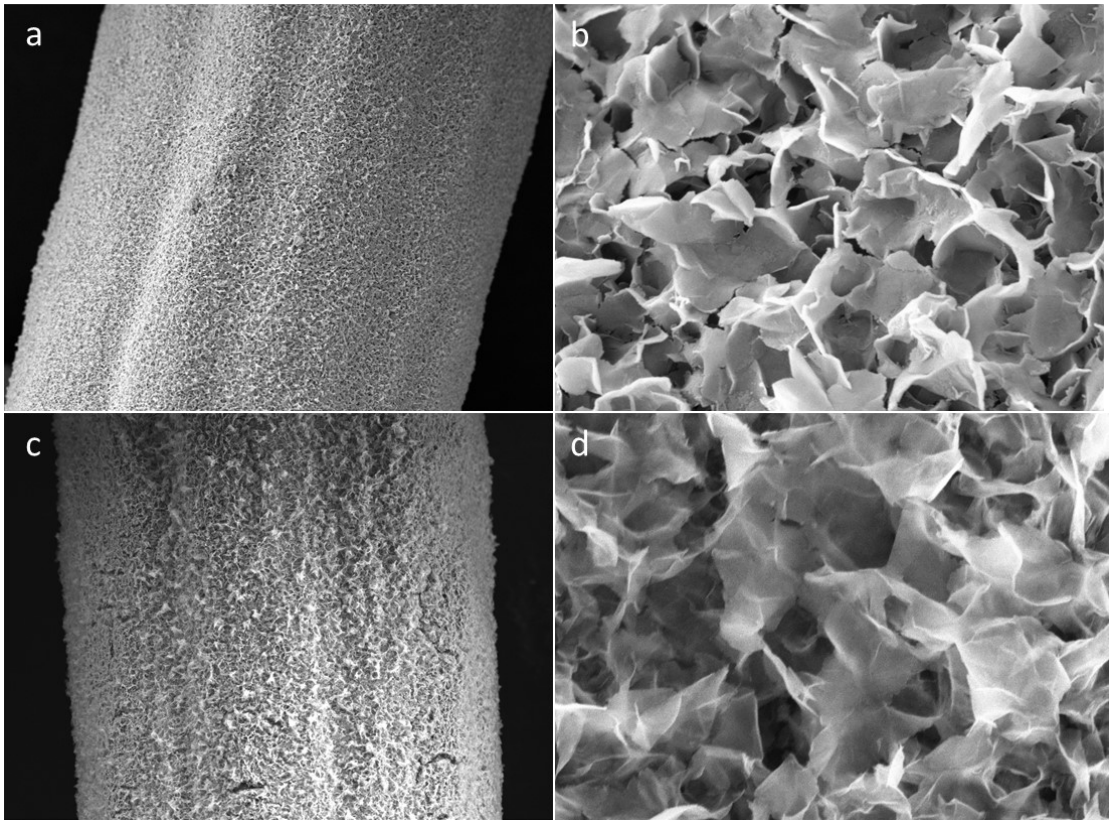

Figure S1. The SEM of CMO (a, b) and CMCO (c, d)

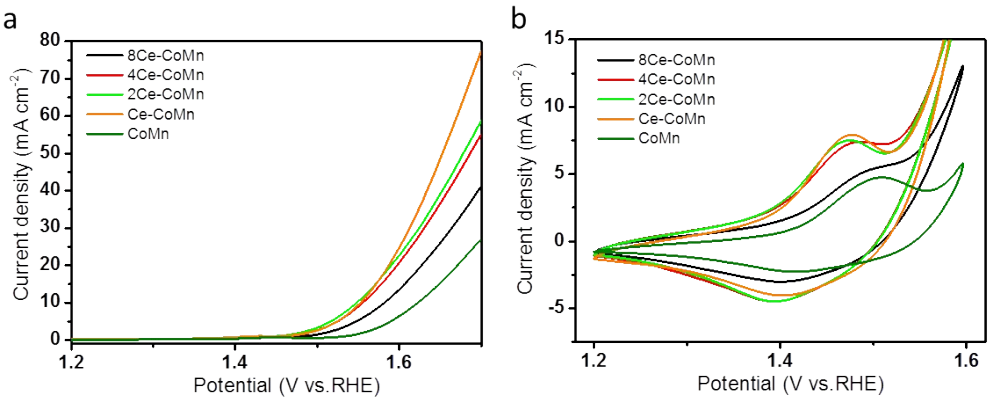

Figure S2. The polarization curves (a) and CV curves (b) of the catalysts with different Ce content used during the electrodeposition. The x in xCe-CoMn represents the x times of Ce is used for the synthesis comparing to that of Ce-CoMn.

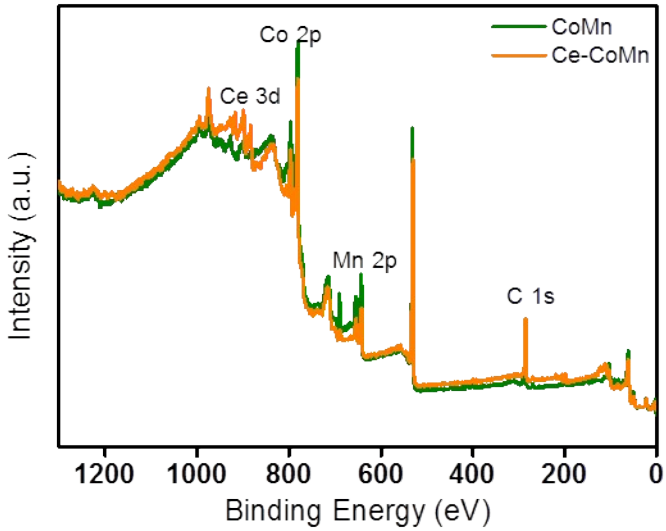

Figure S3. The XPS survey of CMO and CMCO.

Table S1. The comparison of the catalysts with the representative Co- and Mn-based catalysts

Catalysts	**Overpotential**	**References**
$NiCoO_2$@CeO_2	380	Anal. Chem., 2020, 92, 16267.
$MnCo_2O_4$	400	Dalton Trans., 2017, 46, 14382.
RuO_2/CeO_2	350	Int. J. Hydrogen. Energy., 2020, 45,18635
Ce-NiO-E	382	Adv. Funct. Mater. 2018, 1706056
$Co_xNi_{1-x}Fe_2O_4$	381	ACS Appl. Mater. Interfaces 2017, 9, 13132
$MnFe_2O_4$/$NiCo_2O_4$	330	Appl. Catal. B: Environ. 2018, 236, 413–419

NiCo/NLG-270	340	Adv. Mater. 2018, 30, 1800005
β-MnO_2	550	Energy Environ. Sci., 2013, 6, 2222–2232
α -MnO_2	490	J. Am. Chem. Soc., 2014, 136, 11452–11464
Defective δ-MnO_2 nanosheets	320	Adv. Energy Mater. 2017, 7, 1700005.
$AMnO_xH_y$/C	350	J. Energy Chem. 2022, 71, 580-587
Nanowire MnO_2	442	J. Power Sources. 2020,461 228131
$Ni_xCo_{3-x}O4$	337	ACS Appl. Mater. Interfaces 2017, 9, 31777–31785.
Co_3O_4 NC	380	Chem. Commun. 2015, 51, 8066-8069.
CMCO	390	This work
CMO	317	This work

References

1. G. Kresse and J. Furthmüller, *Comput. Mater. Sci.*, 1996, **6**, 15-50.
2. G. Kresse and J. Furthmüller, *Phys. Rev. B*, 1996, **54**, 11169-11186.
3. J. P. Perdew, K. Burke and M. Ernzerhof, *Phys. Rev. Lett.*, 1996, **77**, 3865-3868.
4. S. L. Dudarev, G. A. Botton, S. Y. Savrasov, C. J. Humphreys and A. P. Sutton, *Phys. Rev. B*, 1998, **57**, 1505-1509.
5. Zasada, F., Grybos, J., Indyka, P., Piskorz, W., Kaczmarczyk, J., & Sojka, Z. (2014). The Journal of Physical Chemistry C 118.33 (2014): 19085-19097..
6. J. K. Nørskov, J. Rossmeisl, A. Logadottir, L. Lindqvist, J. R. Kitchin, T. Bligaard and H. Jónsson, *J. Phys. Chem. B*, 2004, **108**, 17886-17892.